International Journal of Modern Physics B
Vol. 27, No. 9 (2013) 1350035 (14 pages)

DOI: 10.1142/S0217979213500355

THERMODYNAMIC QUANTITIES AT HIGH PRESSURES IN THE i AND θ PHASES OF SOLID NITROGEN DEDUCED BY RAMAN FREQUENCY SHIFTS FOR THE INTERNAL MODES IN LITERATURE

H. YURTSEVEN[*,‡] and S. SARITAŞ[*,†]

[*]*Department of Physics, Middle East Technical University, Ankara 06531, Turkey*
[†]*Department of Physics, Bilkent University, Ankara 06800, Turkey*
[†]*sevals@bilkent.edu.tr*
[‡]*hamit@metu.edu.tr*

Received 1 August 2011
Revised 30 July 2012
Accepted 14 January 2013
Published 10 April 2013

The pressure dependence of the Raman frequencies of the internal modes is analyzed ($T = 300$ K) for the phases i and θ of solid nitrogen using the experimental data from the literature. Through the mode Grüneisen parameter, the isothermal compressibility κ_T, thermal expansion α_p and the specific heat $C_p - C_v$ are calculated as a function of pressure using the Raman data in these phases.

We obtain that the α_p varies linearly with the $(1/v)(\partial v/\partial P)_T$ and also that the $C_p - C_v$ varies linearly with the α_p for N_2. Our results show that by means of the analysis given here, the α_p, κ_T and $C_p - C_v$ can be predicted from the Raman frequency shifts for the i and θ phases of solid nitrogen.

Keywords: Internal modes; i phase; θ phase; solid nitrogen.

1. Introduction

Solid nitrogen exhibits various phases under temperature and pressure. At low pressures below 3 kbar and at low temperatures, the α phase occurs with four molecules per unit cell. Above this pressure at 3.5 kbar and at 4.2 K, α phase is transformed into the γ phase.[1] The α phase is stable below 35.4 K and it has a cubic crystal structure with space group $P2_13(T^4)$, whereas the γ phase is tetragonal with a $P4_2/\text{mnm}(D_{4h}^{14})$ space group and there are two molecules per unit cell in this phase.[2] At room temperature, as the pressure is increased to 2 GPa, the supercritical

‡Corresponding author.

fluid solidifies to form the plastic β phase.[3] This high-pressure phase (β) with the hexagonal structure is a highly orientationally disordered phase and it transforms into the orientationally ordered α phase at low temperatures.[4] The solid phases of cubic α phase, hexagonal β phase and tetragonal γ phase, and the fluid phase have been obtained experimentally under various temperatures and pressures as given in the V (molar volume)-T phase diagram.[4,5]

At higher pressures, the other solid phases occur in the solid nitrogen. As a disordered phase with sphere and disk-like molecules which are orientationally distributed between corners and faces of a face centered cubic (fcc) unit cell,[6] the δ phase occurs at high pressures in the solid N_2. As the temperatures decreases or the pressure increases, the δ_{loc}-N_2 phase occurs, where the molecules are partially ordered. With decreasing temperature or increasing pressure, the N_2 molecules become completely ordered in the ε-N_2 phase. At higher pressures of 21–25 GPa at low temperatures,[7] the ε-N_2 is transformed into the ζ-N_2 phase, as also pointed out previously.[8] At room temperature around 20 GPa, another solid phase η-N_2 also exists.[9] Additionally, two more molecular phases of i and θ as the stable phases have been obtained from the measurements of the Raman, infrared and X-ray[8] in solid nitrogen.

Various spectroscopic techniques, mainly Raman, infrared and X-ray have been used to investigate the transitions among the solid phases of N_2. Raman spectra of the α phase,[10,11] α-N_2 and γ-N_2 phases,[12] γ-N_2,[13] α, β and γ phases,[4] δ-N_2, ε-N_2 and η-N_2 phases[14] have been obtained and reported in the literature. Also, by Raman spectroscopy the P–T phase diagrams of solid N_2 have been determined.[8,9,14–17] Far-infrared study on the α-N_2,[18] X-ray measurements for the δ phase,[6,14] the Raman scattering and X-ray diffraction[10,14,16] and also Brillouin scattering[15] studies on the ε-N_2 have been reported in the literature. Another phase η-N_2 has been observed by the Raman[9] and X-ray diffraction[19,20] measurements. Also, the new solid phases of i and θ have been studied using the Raman, infrared and X-ray techniques.[8]

The temperature and pressure dependence of the Raman frequencies and bandwidths of various modes have been studied for the solid phases considered in the solid N_2. In particular, for the α, β and γ phases the detailed Raman spectra of the various lattice and internal modes have been obtained in solid nitrogen at high pressures and low temperatures.[4] We have also studied the Raman frequencies of the lattice and internal modes as a function of temperature in the α and β phases of solid nitrogen in our recent study.[21] Also, the Raman frequencies and the damping constant of the librational mode E_g have been calculated for solid N_2 using anharmonic self energy in our recent study.[22] Recently, the Raman frequency shifts of the internal modes have been measured at high pressures in the range of 20 GPa to 100 GPa at room temperature ($T = 300$ K) in the i-N_2 and θ-N_2 phases.[8] When the ε-N_2 is heated at the pressures of 65–70 GPa, the i-N_2 phase occurs above 750 K.[8] The i-N_2 phase can also be obtained experimentally from the θ-N_2 phase

at ~ 850 K at 69 GPa.[8] It has been pointed out that these two molecular phases (i and θ) have large regions of stability and metastability extending the stable phases of ε and ζ.[8] Both phases (i and θ) are characterized by strong intermolecular interactions and infrared vibron absorption (θ phase). The i phase is dilatomic with orientationally equivalent molecules, which has a kind of lattice consisting of disk-like molecules packed more efficiently in regard to the mixed disk- and spherelike δ-family structures, whereas the θ phase is more complex.[8]

In this study, by analyzing the pressure dependence of the measured Raman frequencies of the internal modes[8] in the i and θ phases, we calculate the isothermal compressibility κ_T through the mode Grüneisen parameter γ_T. From the κ_T calculation, the thermal expansion α_p and the specific heat $C_p - C_v$ are also calculated as a function of pressure in the i and θ phases of solid nitrogen.

Below, in Sec. 2 we give our calculations. Our results are discussed in Sec. 3. Conclusions are given in Sec. 4.

2. Calculations and Results

We calculated here the pressure dependence of the isothermal compressibility κ_T and the thermal expansion α_p from the frequency shifts of the internal Raman mode υ_2 for the phases i and θ of solid N_2. By analyzing the Raman frequencies measured at various pressures[8] for the υ_{2a}, υ_{2b}, υ_{2c} and υ_{2d} for the phase i according to

$$\upsilon = a_0 + a_1 P\,, \tag{1}$$

we were able to calculate the pressure dependence of the isothermal compressibility and the thermal expansion. Table 1 gives the coefficients of a_0 and a_1 from our analysis in phase i. We plot the pressure dependence of the Raman modes υ_{2a}, υ_{2b} and υ_{2c} in Fig. 1 and υ_{2d} in Fig. 2 for the phase i [Eq. (1)]. For the frequency shifts of the Raman modes υ_{2a}, υ_{2b}, υ_{2c} and υ_{2d} at various pressures for a constant temperature ($T = 300$ K) in the θ phase of N_2, this analysis was done by using the pressure dependence of the Raman frequency according to a quadratic relation

$$\upsilon = b_0 + b_1 P + b_2 P^2\,, \tag{2}$$

where b_0, b_1 and b_2 are constants. These coefficients were determined, as given in Table 2. We plot in Fig. 3 the Raman frequencies of the modes υ_{2a}, υ_{2b} and υ_{2c}, and

Table 1. Values of the coefficients a_0 and a_1 in phase i, from the analysis according to Eq. (1) using the experimental frequency data[8] for the Raman modes indicated in solid N_2.

Raman modes	a_0 (cm^{-1})	a_1 (cm^{-1}/GPa)
υ_{2a}	2367.6	1.105
υ_{2b}	2360.3	0.987
υ_{2c}	2367.4	0.797
υ_{2d}	2403.0	0.638

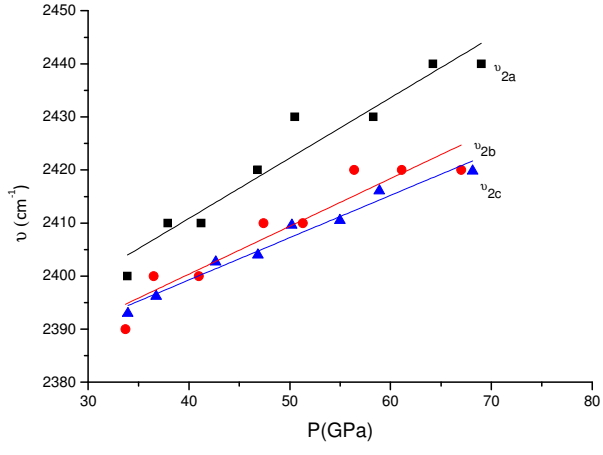

Fig. 1. The experimental Raman frequencies of the υ_{2a}, υ_{2b} and υ_{2c} modes[8] as a function of pressure in the i phase of solid N_2. Solid lines represent Eq. (1) fitted to the experimental data with the coefficients a_0 and a_1 (Table 1).

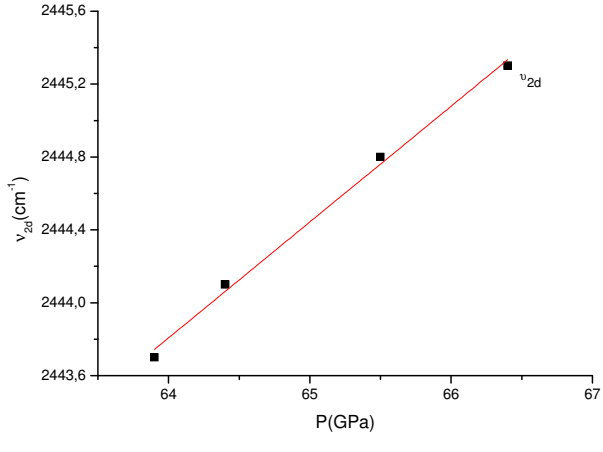

Fig. 2. The experimental Raman frequencies of the υ_{2d} mode[8] as a function of pressure in the phase i of solid N_2. Solid line represents Eq. (1) fitted to the experimental data with the coefficients a_0 and a_1 (Table 1).

in Fig. 4 the υ_{2d} is plotted as a function of pressure ($T = 300$ K) according to Eq. (2) which was fitted to the experimental data[8] for the θ phase of solid nitrogen. Since we aimed to calculate the pressure dependence of the isothermal compressibility κ_T and of the thermal expansion α_p for the phases i and θ using the Raman frequency shifts, the mode Grüneisen parameter γ_j for the jth mode was first determined according to the relation

$$\gamma_j = \left(\frac{1}{\kappa}\right)\left(\frac{1}{\upsilon}\right)\left(\frac{\partial \upsilon_j}{\partial P}\right)_T \tag{3}$$

Table 2. Values of the coefficients b_0, b_1 and b_2 in phase θ from the analysis according to Eq. (2) using the experimental frequency data[8] for the Raman modes indicated in solid N_2.

Raman modes	b_0 (cm^{-1})	b_1 (cm^{-1}/GPa)	$-b_2$ (cm^{-1})/(GPa)^2
υ_{2a}	2292.7	2.169	14
υ_{2b}	2345	1.464	12
υ_{2c}	2335.5	1.923	11
υ_{2d}	2350.5	1.325	8

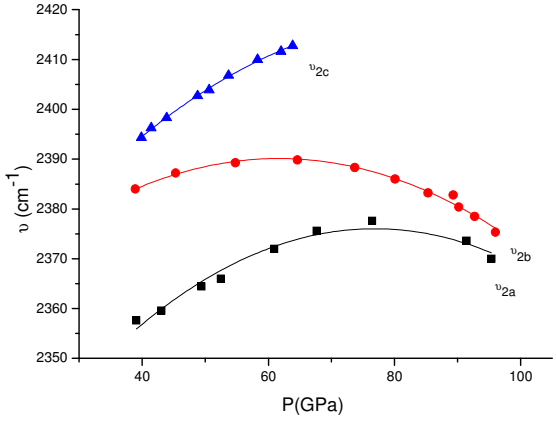

Fig. 3. Experimental Raman frequencies of the υ_{2a}, υ_{2b} and υ_{2c} modes[8] as a function of pressure in the phase θ of solid N_2. Solid curves represent Eq. (2) fitted to the experimental data with the coefficients b_0, b_1 and b_2 (Table 2).

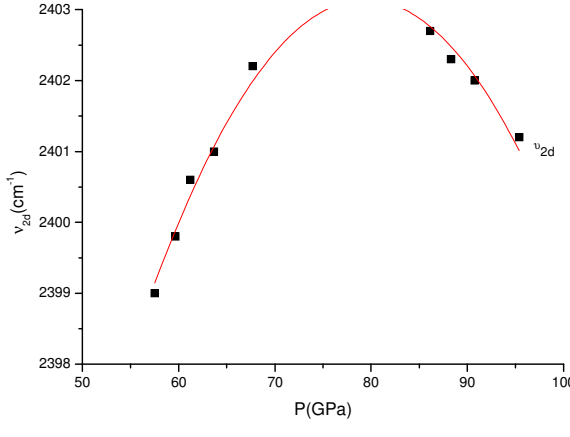

Fig. 4. Experimental Raman frequencies of the υ_{2d} mode[8] as a function of pressure in the phase θ of solid N_2. Solid curve represents Eq. (2) fitted to the experimental data with the coefficients b_0, b_1 and b_2 (Table 2).

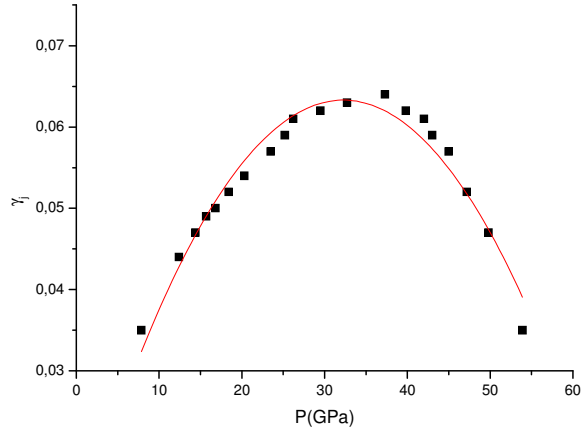

Fig. 5. Grüneisen parameter γ_J of the Raman mode $\upsilon_{2c(2)}$ as a function of pressure for solid N_2.[14] Solid curve represents Eq. (4) fitted to the data[14] with the coefficients a, b and c (Table 3).

Table 3. Values of the coefficients for the pressure dependence of the Grüneisen parameter[14] of the Raman mode indicated in solid N_2 according to Eq. (4).

Raman mode	$a \times 10^{-3}$	$b \times 10^{-3}$ (GPa)$^{-1}$	$-c \times 10^{-5}$ (GPa)$^{-2}$
$\upsilon_{2c(2)}$	9.3	3.3	5

for the internal mode $\upsilon_{2c(2)}$. The isothermal Grüneisen parameter for this mode[14] at various pressures is plotted in Fig. 5. We then calculated κ_T and α_p as a function of pressure for the phases i and θ of solid N_2. The pressure dependence of the mode Grüneisen parameter was analyzed according to a quadratic function given by:

$$\gamma_T = a + bP + cP^2\,, \tag{4}$$

where a, b and c are constants. Values of these constants for the $\upsilon_{2c(2)}$ mode are given in Table 3. Thus, using the pressure dependence of the frequency shifts $(1/\upsilon)(\partial\upsilon/\partial P)_T$ and of the mode Grüneisen parameter γ_T for the internal mode υ_2, we calculated the isothermal compressibility κ_T at various pressures according to Eq. (3). The pressure dependence of κ_T was then used to calculate the pressure dependence of the thermal expansion α_p through the thermodynamic relation

$$\left(\frac{\alpha_p}{\kappa_T}\right) = \left(\frac{dP}{dT}\right), \tag{5}$$

for the phases i and θ of solid N_2. In Eq. (5), dP/dT is the slope of the phase line in the P–T phase diagram. We determined this slope from the phase line between the phases ε and ζ in the P–T phase diagram of solid N_2, as measured experimentally.[8] The temperature dependence of the pressure was expressed as:

$$P = c_0 + c_1 T \tag{6}$$

Table 4. Values of the coefficients c_0 and c_1 according to Eq. (6) for the phases indicated in solid N_2.

Phases	$-c_0$ (GPa)	c_1 (GPa/K)	dP/dT (GPa/K)
$\varepsilon - \zeta$	1.65	0.20	0.20

with the coefficients c_0 and c_1, as given in Table 4. This gives the slope value of $dP/dT = 0.20$ GPa/K for the phases between ε and ζ.

Finally, we evaluated the pressure dependence of the thermal expansion α_p using the values of the isothermal compressibility κ_T which were obtained from the Raman frequency shifts [Eq. (3)] as stated above and the slope (dP/dT) value for the phases i and θ of solid N_2. In Fig. 6 we plot our calculated α_p as a function of the frequency shifts $(1/\gamma_T)(1/\upsilon)(\partial\upsilon/\partial P)_T$ at various pressures for the internal modes υ_{2a}, υ_{2b} and υ_{2d} and in Fig. 7 for υ_{2c} for the phase i of solid N_2. Similar plots of α_p versus $(1/\gamma_T)(1/\upsilon)(\partial\upsilon/\partial P)_T$ for the υ_{2a} (Fig. 8), υ_{2b} (Fig. 9) and for the υ_{2c} and υ_{2d} (Fig. 10) modes for the θ phase of solid N_2. All the plots (Figs. 6–10) were obtained according to the spectroscopic modification of the Pippard relation

$$\alpha_p = \left(\frac{1}{\gamma_T}\right)\left(\frac{dP}{dT}\right)\left(\frac{1}{\upsilon}\right)\left(\frac{\partial\upsilon}{\partial P}\right)_T + \left(\frac{1}{V}\right)\left(\frac{dV}{dT}\right). \tag{7}$$

In Eq. (7) γ_T is the isothermal mode Grüneisen parameter and dV/dT is the variation of the volume with the temperature. Equation (7) can be obtained from the Pippard relation:

$$\alpha_p = \left(\frac{dP}{dT}\right)\kappa_T + \left(\frac{1}{V}\right)\left(\frac{dV}{dT}\right), \tag{8}$$

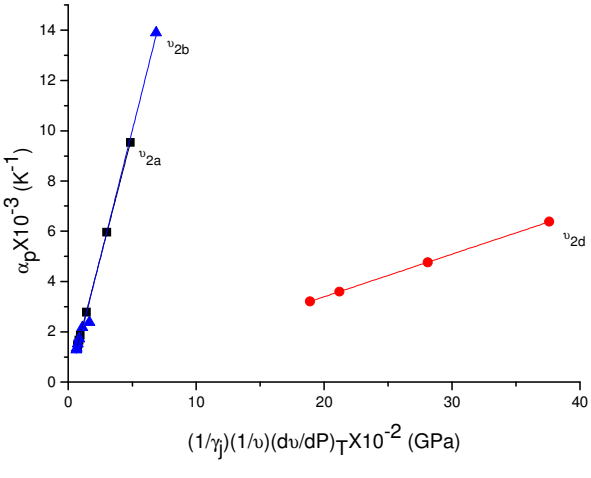

Fig. 6. Thermal expansion α_p as a function of the frequency shift for the Raman modes of υ_{2a}, υ_{2b} and υ_{2d} according to Eq. (7) for the phase i of the solid N_2.

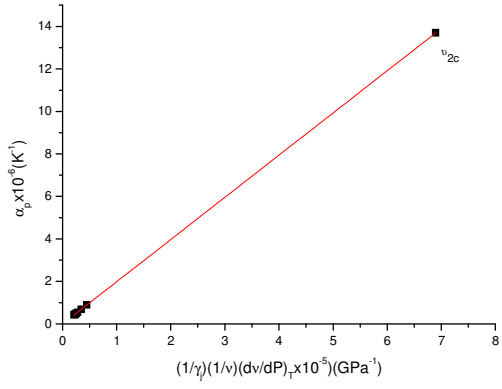

Fig. 7. Thermal expansion α_p as a function of the frequency shift for the Raman mode υ_{2c} according to Eq. (7) for the phase i of the solid N_2.

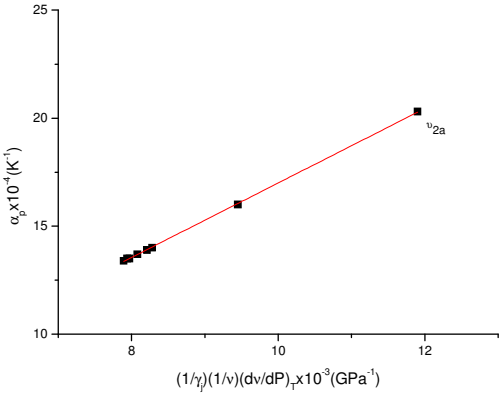

Fig. 8. Thermal expansion α_p as a function of the frequency shift for the Raman mode υ_{2a} according to Eq. (7) for the phase θ of solid N_2.

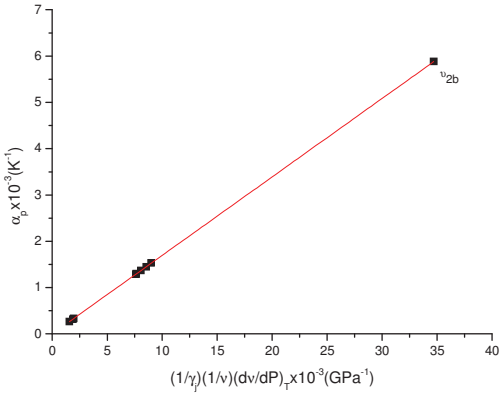

Fig. 9. Thermal expansion α_p as a function of the frequency shift for the Raman mode υ_{2b} according to Eq. (7) for the phase θ of solid N_2.

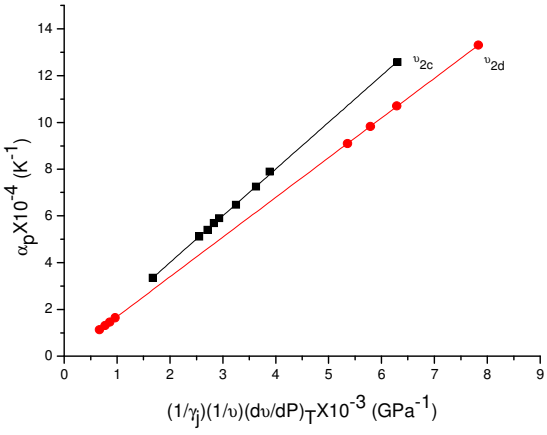

Fig. 10. Thermal expansion α_p as a function of the frequency shift for the Raman modes of υ_{2c} and υ_{2d} according to Eq. (7) for the phase θ of solid N_2.

through the Eq. (3). When α_p is plotted as a function of $(1/\upsilon)(\partial\upsilon/\partial P)_T$, we should get a straight line as given in Figs. 6–10 for the phases i and θ of solid N_2. The slope dP/dT can then be extracted from those plots.

Calculation of the thermal expansion α_p led us to evaluate the pressure dependence of the specific heat C_p according to the thermodynamic relation:

$$C_p - C_v = \frac{TV\alpha_p^2}{\kappa_T} \tag{9}$$

or using Eq. (5),

$$(C_p - C_v) = TV\left(\frac{dP}{dT}\right)\alpha_p\,. \tag{10}$$

Since we calculated the pressure dependence of the isothermal compressibility κ_T using the frequency shifts $(1/\upsilon)(\partial\upsilon/\partial P)_T$ of the Raman modes studied and the Grüneisen parameter γ_T [Eq. (3)], the difference in the specific heat, $C_p - C_v$ was evaluated [Eq. (9)]. Using the pressure dependence of the frequency shifts for the Raman modes of υ_{2a}, υ_{2b}, υ_{2c} and υ_{2d}, we calculated $(C_p - C_v)/V$ as a function of α_p for various pressures in the phases i and θ of solid nitrogen. We give our plots of $(C_p - C_v)/V$ versus α_p using the Raman frequencies of υ_{2a} and υ_{2b} (Fig. 11), the υ_{2c} (Fig. 12) and the υ_{2d} (Fig. 13) for the phase i of solid N_2. Similar plots of $(C_p - C_v)/V$ versus α_p are given using the Raman frequencies of υ_{2a} (Fig. 13) and, the υ_{2c} and υ_{2d} (Fig. 14) modes for the phase θ of solid nitrogen. The frequency shifts of the υ_{2b} mode did not give any linear variation of C_p with the α_p for this phase of solid N_2. They are plotted according to Eq. (10) and the slope value was obtained as $dP/dT = 0.20$ GPa/K at $T = 297$ K for the phases i and θ of solid nitrogen.

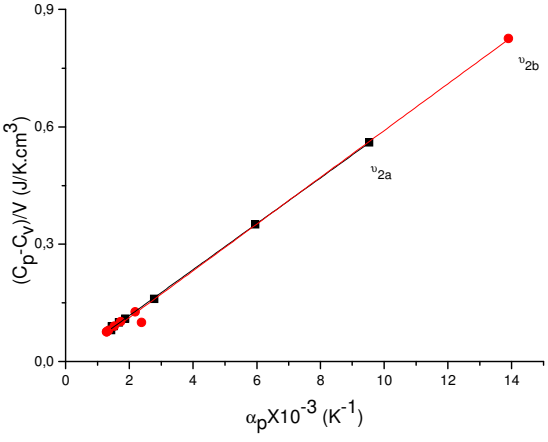

Fig. 11. The difference in the specific heat per unit volume as a function of the thermal expansion α_p according to Eq. (10) where the Raman frequencies of the υ_{2a} and υ_{2b} modes were used in the phase i of solid N_2.

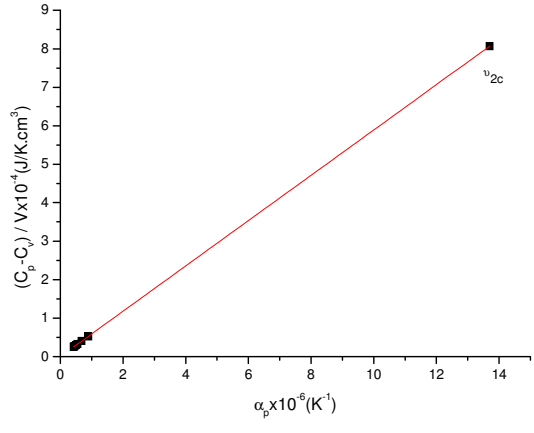

Fig. 12. The difference in the specific heat per unit volume as a function of the thermal expansion α_p according to Eq. (10) where the Raman frequencies of the υ_{2c} mode were used in the phase i of solid N_2.

3. Discussion

The Raman frequency shifts $(1/\upsilon)(\partial\upsilon/\partial P)_T$ were related to the thermal expansion α_p for the internal modes of υ_{2a}, υ_{2b}, υ_{2c} and υ_{2d}, and the linear relations were obtained in the phases i and θ of solid N_2, as shown in Figs. 6–10. Linear variation of the specific heat $C_p - C_v$ with the α_p was also obtained by using the Raman frequencies for the internal modes of υ_{2a}, υ_{2b}, υ_{2c} and υ_{2d}, as shown in Figs. 11–14. Value of the slope was obtained from those linear plots as $dP/dT = 0.20$ GPa/K which was also obtained from the experimental T–P phase diagram[8] between the phases ε and ζ (Table 4). This is expected since we used experimental dP/dT value

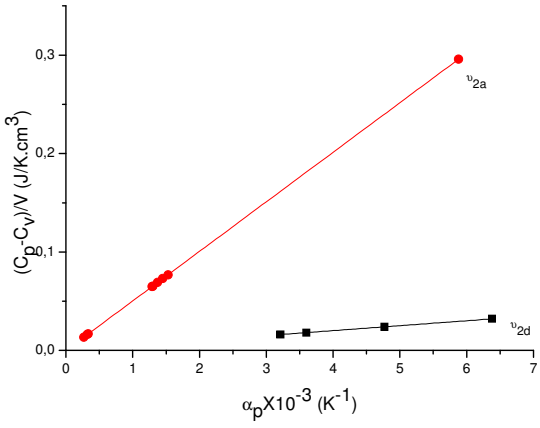

Fig. 13. The difference in the specific heat per unit volume as a function of the thermal expansion α_p according to Eq. (10) where the Raman frequencies of the υ_{2d} mode (phase i) and of υ_{2a} mode (phase θ) of solid N_2 were used.

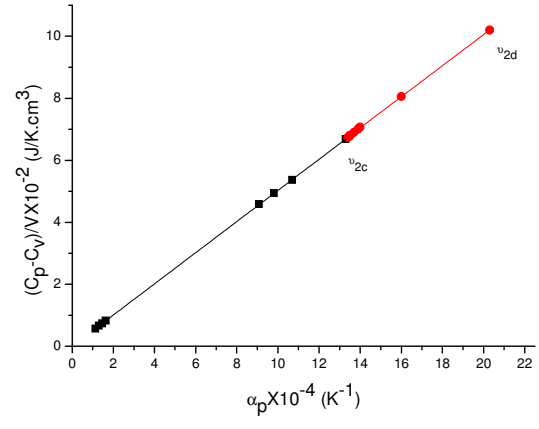

Fig. 14. The difference in the specific heat per unit volume as a function of the thermal expansion α_p according to Eq. (10) where the Raman frequencies of the υ_{2c} and υ_{2d} modes were used for the phase θ of solid N_2.

to calculate the pressure dependence of the thermal expansion α_p [Eq. (5)] and the specific heat $C_p - C_v$ [Eq. (10)].

Linear variation of the α_p with the $(1/\upsilon)(\partial\upsilon/\partial P)_T$ and also a linear variation of $C_p - C_v$ with the α_p, giving the same dP/dT value are based on the best fit of Eqs. (1) and (2) for the i and θ phases, respectively, to the experimental Raman frequencies of the internal modes υ_{2a}, υ_{2b}, υ_{2c} and υ_{2d}, as shown in Figs. 1–4. In fact, the Raman frequencies for the modes υ_{2a}, υ_{2b} and υ_{2c} (Fig. 1) and υ_{2d} mode (Fig. 2) for the phase i are not linearly dependent on pressure, instead that dependence is nonlinear, as observed experimentally.[8] However, within the pressure interval considered here, a linear dependence of the Raman frequency on the pressure [Eq. (1)]

can be taken as a good approximation for the internal modes studied whereas this is not the case for the pressure dependence of the Raman modes of υ_{2a}, υ_{2b}, υ_{2c} (Fig. 3) and υ_{2d} (Fig. 4) for the phase θ of solid N_2. Non-linear (quadratic) dependence of the Raman frequencies on the pressure was obtained according to Eq. (2), as stated above. Furthermore, we fitted Eq. (4) as a quadratic relation to the experimental data for the pressure dependence of the mode Grüneisen parameter for the Raman mode of $\upsilon_{2c(2)}$ as shown in Fig. 5. We assumed here that the pressure dependence of the Raman modes υ_{2a}, υ_{2b}, υ_{2c} and υ_{2d} was in the same functional form as the $\upsilon_{2c(2)}$ whose mode Grüneisen parameter [Eq. (4)] was obtained at various pressures.[14] So, this assumption was also reasonable to construct linear variations of α_p versus $(1/\upsilon)(\partial\upsilon/\partial P)_T$ and $C_p - C_v$ versus α_p using the Raman frequencies for the internal modes of υ_{2a}, υ_{2b}, υ_{2c} and υ_{2d}.

As in Figs. 1–4, the pressure dependence of the Raman frequencies of vibron modes (υ_1 and υ_2) is different for the phases of i-N_2 and θ-N_2. This is due to different structures of both phases. As also indicated in previous Raman studies,[9,23,24] some of the intramolecular vibrations soften when the pressure increases, which can be related to the weakening of intramolecular bonding or to the increase in vibrational coupling.[25] It has been indicated that there is a more pronounced Raman and IR softening of the vibron bands of θ nitrogen as compared to the i nitrogen.[8] For the lattice modes of θ nitrogen, it has been observed that they are very sharp and high in intensity in comparison with i nitrogen.[8] This indicates that there is a complete ordering in θ nitrogen, whereas i nitrogen, has to some degree static and dynamic orientational disorder due to weak and broad bands.[8] In the disorder i nitrogen, vibrational coupling does not exist and due to increasing intermolecular interaction branching of vibrational modes and increasing of separation between them with the pressure taking place.[8] As also pointed out in the previous study,[8] the i phase has one type of site symmetry for the molecules and many vibrational modes arise from a unit cell of eight molecules (branching of vibrational modes), whereas for the θ phase there are two different site symmetries. Since the vibrational frequency depends on the axial force acting on the molecule which depends on its orientation,[26] the molecules in the ordered θ phase feel a constant crystal field and with a fixed orientation their vibrational lines become narrow, as also pointed out previously.[27]

Regarding the pressure dependence of the Raman mode υ_{2d} (Fig. 4) for the phase θ, one needs more experimental data for a better analysis according to Eq. (1) or a quadratic function can be considered. For the other Raman modes of υ_{2a}, υ_{2b} and υ_{2c} (Fig. 1), some other functional forms rather than a linear dependence [Eq. (1)] can be employed. Experimental measurements for the Raman frequencies of the υ_{2a}, υ_{2b}, υ_{2c} and υ_{2d} are needed at various pressures ($T = 300$ K) with many data points for the α_p versus $(1/\upsilon)(\partial\upsilon/\partial P)_T$ and $C_p - C_v$ versus α_p plots in the phases of i and θ of solid N_2. This can give a better test for the validity of the Pippard relations [Eqs. (7) and (10)] using the Raman frequencies of the modes studied here in the pressure range of the phases i and θ of N_2.

Finally, from the quadratic dependence of the mode Grüneisen parameter on the pressure [Eq. (4)] we obtained that the value γ_T varies from ~ 0.01 ($P = 0$) to 0.04 for the internal mode $\upsilon_{2c(2)}$ in the pressure range (0–60 GPa) studied here for the solid nitrogen. Those values of the mode Grüneisen parameter for the $\upsilon_{2c(2)}$ internal mode are reasonable at high pressures. Our values can be compared with the values of the internal modes that vary from 0.01 to 0.06 in phase I of benzene,[22] which is also expected from a molecular crystal[23] such as solid N_2 studied here.

4. Conclusions

The Raman frequencies of the internal modes were studied as a function of pressure using the experimental data for the phases i and θ of solid N_2. The pressure dependence of the Grüneisen parameter for the internal mode was also analyzed using the experimental data.

Through the Raman frequency shifts and the mode Grüneisen parameter, the thermodynamic quantities of the isothermal compressibility, thermal expansion and the specific heat were calculated at various pressures ($T = 300$ K) for the phases i and θ of solid nitrogen. Linear plots of the thermal expansion against the Raman frequency shifts and the specific heat against the thermal expansion were obtained, and the experimental value of the slope dP/dT was deduced for the phases i and θ of N_2. This shows that the Raman frequency shifts can be related to the thermodynamic quantities and those quantities can be predicted reasonably well for the phases i and θ of solid nitrogen.

References

1. C. A. Swenson, *J. Chem. Phys.* **23**, 1963 (1955).
2. R. L. Mills and A. F. Schuch, *Phys. Rev. Lett.* **23**, 1154 (1969).
3. D. A. Young *et al.*, *Phys. Rev. B* **35**, 5353 (1987).
4. F. D. Medina and W. B. Daniels, *J. Chem. Phys.* **64**, 150 (1976).
5. A. F. Schuch and R. L. Mills, *J. Chem. Phys.* **52**, 6000 (1970).
6. D. Cromer *et al.*, *Acta Crystallogr. Sect. B* **37**, 8 (1981).
7. D. Schiferl, S. Buchsbaum and R. L. Mills, *J. Phys. Chem.* **89**, 2324 (1985).
8. E. Gregoryanz *et al.*, *Phys. Rev. B* **66**, 224108 (2002).
9. R. Reichlin *et al.*, *Phys. Rev. Lett.* **55**, 1464 (1985).
10. A. Anderson, T. S. Sun and M. C. A. Donkersloot, *Can. J. Phys.* **48**, 2265 (1970).
11. P. M. Mathai and E. J. Allin, *Can. J. Phys.* **49**, 1973 (1971).
12. M. M. Thiery *et al.*, *J. Chem. Phys.* **59**, 4559 (1973).
13. F. D. Medina and W. B. Daniels, *J. Chem. Phys.* **59**, 6175 (1973).
14. H. Schneider *et al.*, *J. Chem. Phys.* **96**, 8046 (1992).
15. M. Grimsditch, *Phys. Rev. B* **32**, 514 (1985).
16. R. L. Mills, B. Olinger and D. T. Cromer, *J. Chem. Phys.* **84**, 2837 (1986).
17. T. Westerhoff, A. Wittig and R. Feile, *Phys. Rev. B* **54**, 14 (1996).
18. F. D. Medina, *J. Chem. Phys.* **77**, 4785 (1982).
19. A. P. Jephcoat *et al.*, *Bull. Am. Phys. Soc.* **33**, 522 (1988).
20. H. Olijnyk, *J. Chem. Phys.* **93**, 8968 (1992).
21. H. Yurtseven and T. Tunay, *Int. J. Mod. Phys. B* **24**, 6069 (2010).

22. H. Yurtseven and M. Kurt, *Int. J. Mod. Phys. B* **25**, 3679 (2011).
23. P. M. Bell, H. K. Mao and R. J. Hemley, *Physica* (*Amsterdam*) **139B–140B**, 16 (1986).
24. H. Olijnyk and A. P. Jephcoat, *Phys. Rev. Lett.* **83**, 332 (1999).
25. A. F. Goncharov *et al.*, *Phys. Rev. Lett.* **85**, 1262 (2000).
26. M. I. M. Scheerboom and J. A. Schouten, *J. Chem. Phys.* **105**, 2553 (1996).
27. L. Tassini, F. Gorelli and L. Ulivi, *J. Chem. Phys.* **122**, 074701 (2005).
28. M. M. Thiery and J. M. Leger, *J. Chem. Phys.* **89**, 4255 (1988).
29. R. Zallen, *Phys. Rev. B* **9**, 4485 (1974).